



Peeling behavior of a film on inner surface of a tube

Yunqiang Hu^a, Jinsong Leng^b, Fei Jia^{a,*}, Yanju Liu^{a,*}

^a Department of Astronautical Science and Mechanics, Harbin Institute of Technology (HIT), P.O. Box 301, No. 92 West Dazhi Street, Harbin 150001, China

^b Center for Composite Materials and Structures, Science Park of Harbin Institute of Technology (HIT), P.O. Box 3011, No. 2 YiKuang Street, Harbin 150080, China



ARTICLE INFO

Article history:

Received 8 July 2022

Received in revised form 19 September 2022

Accepted 18 November 2022

Available online 21 November 2022

Keywords:

Elastic film

Adhesion of curved surface

Zero peeling angle

Displacement control loading mode

ABSTRACT

Adhesion behavior of elastic films is a common phenomenon in many biological processes and industrial applications. Current film peeling theories and adhesion property testing methods are mostly limited to flat peeling cases. In this paper, peeling behaviors of elastic films on tubular surfaces are studied through theoretical analysis and finite element simulation. Based on the theory of non-linear elasticity, mechanical behaviors of cylindrical films under finite deformation are investigated and the total strain energy is obtained through dimensional analysis. Furthermore, an analytical expression for energy release rate of an axisymmetric crack is derived. By balancing with the density of energy, the length of crack varies linearly with the axial stretch. Finite element method is adopted to simulate the peeling process of a film and the results agree well with theoretical predictions. Our peeling method, which decouples the influence of surface frictions that commonly cannot be ignored in conventional one degree of freedom peeling setups, represents a new, useful, and easy-to-implement strategy to study elastic film peeling behaviors. Beyond this, the model and the results are also useful for measuring adhesion properties of soft films.

© 2022 Elsevier Ltd. All rights reserved.

1. Introduction

Adhesion behavior of soft matter is an ubiquitous phenomenon in both nature and engineering practices, which may have beneficial or catastrophic consequences. For instance, cell-to-cell adhesion is able to transmit extracellular or intracellular forces [1] which can maintain the normal function of organisms. Changes in cell adhesion may lead to a variety of diseases, including arthritis, cancer and atherosclerosis [2–4]. Another example is that marine animal attachment to hull surfaces results in increased weights and maintenance costs for marine vessels [5]. Understanding soft matter adhesion is also important in deicing or anti-icing [5–7], implantable biomedical devices [8], and flexible electronics [9].

Soft matter adhesion has been usually studied by planar peeling methods. Kendall [10] theoretically studied film peeling from rigid substrates utilizing the crack energy criterion, which has been widely used to study film peeling behaviors. For example, a non-linear film peeling model considering the effect of pre-straining was proposed by Molinari et al. [11]. Besides, film plastic/viscoelastic peeling behaviors were modeled and numerically investigated [12–15]. In addition, effects of surface topographies were investigated [16–18].

Very few attempts have been made to consider film peeling from curved surfaces which are more common in nature and practical applications. Thin film peeling from partial cylinder surfaces was studied by Kruglova et al. [19], and shapes of the tears can be observed by adjusting substrate curvatures. Brely et al. developed a numerical model to simulate the peeling of adhesive tape-substrate system, and substrate roughness, patterning, curvature, and deformability were considered [20]. The adhesive behavior of bonded pipes with curved-surface lap joints was experimentally analyzed [21]. In a word, it is still an unmet challenge for successful theoretical analysis of elastic film peeling from tubular surfaces.

In this work, elastic film peeling from inner tubes, as a typical curved surface, is studied. As shown in Figs. 1(a) and (b), the film is initially adhered to the inner surface of a tube and then is peeled under vertical stretch with fixed radius at the top end. The angle between the loading direction and the axis of symmetry is zero. If the displacement load with zero peeling angle is applied on a film attached to a flat substrate, it will cause difficulties in theoretical analysis. The presence of frictional sliding at the interface between the detached film and the substrate leads to significantly higher peeling forces [22]. Fixed non-zero angle peeling methods [22,23] are usually used to avoid the coupling of friction during peeling, but these methods may bring complicated experimental setup.

* Corresponding authors.

E-mail addresses: feijia@hit.edu.cn (F. Jia), yj_liu@hit.edu.cn (Y. Liu).

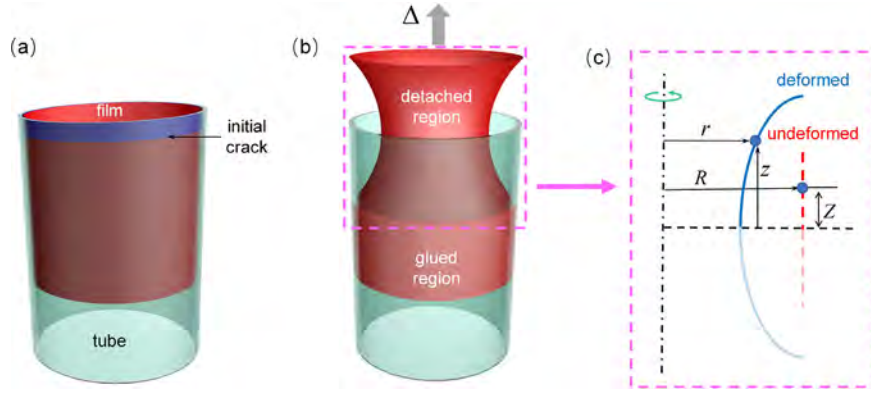


Fig. 1. Schematics of film peeling: (a) Film is bonded on a tube with an initial crack before stretch. (b) Vertical displacement loading is applied at film top end with fixed radius. The film can be divided into detached and glued regions with crack line in-between. (c) In axisymmetric model of half detached film, two coordinate systems, (R, Z) and (r, z) , are used to describe the undeformed and deformed film, respectively.

Tubular zero angle peeling methods is a simple setup that can decouple the influence of surface frictions that commonly cannot be ignored in conventional one degree of freedom peeling set-ups. As shown in Fig. 1(b), axial stretching of an elastic film bonded to an inner tube causes finite deformation circumferential shrinkages. A peeling angle at the crack tip is automatically generated due to necking[24–26]. Once the film is peeled off from the tube, detached part of the film is free from the tube, so there is no friction between the film and the tube. From this point, tubular peeling naturally decouples the peeling behavior from the frictional sliding under a very simple displacement loading. Therefore, tubular peeling may have experimental significance in measuring the adhesion property of film–substrate interfaces.

This paper is organized as follows. Theoretical modeling of tubular films under uni-axial stretching is completed in Sections 2 and 3. In Section 4, relationship between loading displacements and peeling behaviors is studied. The theoretical results are compared with the finite element(FE) simulation, and a new method to measure the adhesion properties of the film–substrate system is proposed in Section 5.

2. Theory

Based on the theory of non-linear elasticity about films [27,28], we establish an axisymmetric model to analyze the deformation of the film, as shown in Fig. 1(c). Because the thickness of the film is much smaller than its radius, the deformation difference along thickness direction can be neglected, and the entire film can be represented by its midsurface. In reference configuration, a point of coordinate on the midsurface of the film can be written as

$$\mathbf{X} = R\mathbf{e}_r + Z\mathbf{e}_z, \quad 0 \leq Z \leq \frac{L}{2}, \quad (1)$$

where $\{\mathbf{e}_r, \mathbf{e}_\theta, \mathbf{e}_z\}$ are the unit vectors of the cylindrical coordinate with $\{r, \theta, z\}$ as shown in Fig. 1(c), R is the initial radius of film and L, Z are the length and z -directional coordinate of the film midsurface in the reference configuration, respectively. Since the upper and lower parts of the film are symmetrical, we analyze half of the model illustrated in Fig. 1(c). The coordinate of a point (\mathbf{X}) in reference configuration mapping into the current configuration can be written as

$$\mathbf{x} = r(Z)\mathbf{e}_r + z(Z)\mathbf{e}_z. \quad (2)$$

As stated in literature [28], the principle stretch ratios of tangential, azimuthal, and normal directions are

$$\lambda_s = \sqrt{r'^2 + z'^2}, \quad \lambda_\theta = \frac{r}{R}, \quad \lambda_n = \frac{h}{H}, \quad (3)$$

where a prime denotes differentiation with respect to Z , and H and h are the thickness of film in reference and current configurations, respectively. The angle between tangential direction and axial direction, ξ , can be expressed as

$$\cos \xi = \frac{z'}{\lambda_s}, \quad (4)$$

which reflects the necking extent. The equilibrium equations in the tangential, azimuthal, and normal directions are respectively given by [28]

$$\begin{aligned} (rT_s)' - r'T_\theta &= 0, \\ \frac{\partial(rT_\theta)}{\partial\theta} &= 0, \\ \kappa_s T_s + \kappa_\theta T_\theta &= 0, \end{aligned} \quad (5)$$

where T_s and T_θ are the principal stress resultants per unit length in tangential and azimuthal directions, respectively. The second equation in Eq. (5) is automatically satisfied due to the axisymmetric feature of our model. κ_s and κ_θ are the principal curvatures in the tangential and azimuthal directions, respectively,

$$\kappa_s = \frac{1}{r'} \left(\frac{z'}{\sqrt{r'^2 + z'^2}} \right)', \quad \kappa_\theta = \frac{z'}{r\sqrt{r'^2 + z'^2}}. \quad (6)$$

Now we derive T_s and T_θ from the constitutive model. A commonly used neo-Hookean model is chosen to study the mechanical behavior of rubber films under large deformation. The strain-energy function of neo-Hookean model is [27]

$$W(\lambda_\theta, \lambda_s) = \frac{\mu}{2} \left(\lambda_\theta^2 + \lambda_s^2 + \frac{1}{\lambda_\theta^2 \lambda_s^2} - 3 \right), \quad (7)$$

where μ is shear modulus and the incompressibility of the material model ensures that $\lambda_s \lambda_\theta \lambda_n = 1$. The principle stress resultants per unit length in the deformed film are defined as [28]

$$T_s = \frac{H}{\lambda_\theta} \frac{\partial W}{\partial \lambda_s}, \quad T_\theta = \frac{H}{\lambda_s} \frac{\partial W}{\partial \lambda_\theta}. \quad (8)$$

3. Film stretching

In this section, we investigate the shape of film after deformation through theoretical analysis and finite element simulation. The results of present section will be used to analyze the peeling process of film from a tube (to be presented in Section 4). During theoretical procedures, we set $H = 1, \mu = 1$ and $R \geq 10H$.

As the upper and lower parts are symmetrical with respect to the transverse section $Z = 0$ in Fig. 1(c), the boundary conditions for r' and z at $Z = 0$ are all zero. In addition, film is

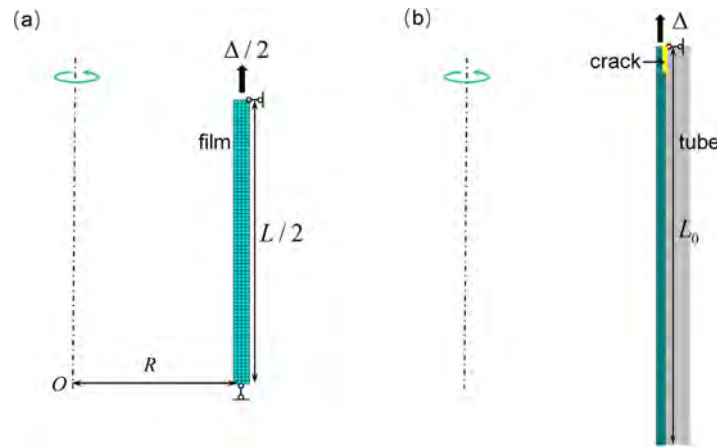


Fig. 2. Geometry and mesh of axisymmetric finite element models: (a)stretching of film, (b) peeling process of film from a tube.

stretched under displacement loading with fixed radius at both ends. Therefore boundary conditions can be summarized as

$$z(0) = 0, \quad r'(0) = 0, \quad r\left(\frac{L}{2}\right) = R, \quad z\left(\frac{L}{2}\right) = \frac{\Delta}{2}. \quad (9)$$

Similar to the theoretical analysis, an axisymmetric model with boundary conditions of Eq. (9) for half film is performed by ABAQUS software to study the film stretch. As illustrated in Fig. 2(a), 8-node biquadratic axisymmetric quadrilateral elements with hybrid and reduced integration are used in this simulation and the size of element is 0.25×0.25 .

Through dimensional analysis, the relationship of multiple physical quantities is studied. Strain energy E_e of the deformed film is related to μ , H , R , L and the displacement of the top of film Δ . E_e can be expressed as

$$E_e = \mu H \Delta^2 f\left(\frac{L}{\Delta}, \frac{R}{\Delta}\right). \quad (10)$$

The relationship between E_e and R is ascertained by extensive theoretical analysis and finite element simulations. It can be found that E_e varies linearly with R (details can be found in Section 5) and Eq. (10) can be further written as

$$E_e = \mu H R \Delta f(\eta), \quad (11)$$

where $\eta = L/\Delta$.

4. Tubular film peeling behavior

In present section, we study the process of film peeling from a tube. Lower part of film is bonded to a rigid tube and the rest part is naturally lied on the tube. When stretching film using the displacement loading denoted by Δ , the energy equilibrium equation of the film-tube system can be written as

$$E_t = E_e + E_s, \quad (12)$$

where E_t is the external work and E_s is the surface energy. The crack expands during deformation causing the energy change and the derivative of Eq. (12) to the crack area A gives the energy release rate G ,

$$G = \frac{\partial E_s}{\partial A} = \frac{\partial(E_t - E_e)}{\partial A}. \quad (13)$$

Quasi-static based displacement controlled loading mode is used to study the film peeling from a tube. Crack propagation stops when the total energy of the system reaches the minimum

value. Due to axisymmetric deformation, we have $dA = 2\pi R dL$. Eq. (13) can further be written as

$$G = -\frac{1}{2\pi R} \frac{\partial E_e}{\partial L}. \quad (14)$$

Substituting Eq. (11) into Eq. (14), we obtain

$$f'(\eta) = -\frac{2\pi}{\mu H} G. \quad (15)$$

For simplification, G is assumed as a constant. If $f'(\eta)$ is a monotonous function of η , a constant value η_0 can be determined from Eq. (15), that is $L = \eta_0 \Delta$, indicating that the crack length L varies linearly with the applied displacement Δ during peeling process.

This interesting relationship between L and Δ will also be verified by FE simulations with similar material model, mesh elements, boundary conditions, and simulation procedure used in Section 3, as shown in Fig. 2(b). Besides, we use the Virtual Crack Closure Technique (VCCT) criterion as the crack propagation criterion, with the key parameters $G_I = G_{II} = 0.1$, $G_{III} = 0$, and $\gamma = 1$, to define the interaction between film and the inner tube. In all the film peeling simulations, we create an initial crack with the same length of H . The initial bonded length is set long enough to ensure a complete capture of elastic film peeling process.

5. Results and discussions

Theoretical film deformation under stretching can be solved from Eqs. (5) and (9), while film peeling behaviors can be obtained from Eq. (15). All theoretical results are compared with numerical simulations in this section.

5.1. Film stretching results

The deformed film profile obtained from FE simulation with $\Delta = 20$, $R = 20$, and $L = 40$ is illustrated in Fig. 3(a) where necking can be observed. Fig. 3(b) shows the comparisons of the film deformation between theoretical analysis and FE simulations under different displacement loading conditions $\Delta/R = 0.25, 0.5, 0.75, 1.0$, where $R = 20$ and $L = 40$. The theoretical results of normalized radius \tilde{r} and normalized vertical coordinate \tilde{z} are in well agreement with FE simulation results, where $\tilde{z} = z/R$ and $\tilde{r} = r/R$, indicating the appropriateness of the proposed theoretical model to some extent.

Fig. 3(c) shows the normalized radius \tilde{r}_h at the throat $Z = 0$ and the angle ξ_h at the top end $Z = L/2$ varying with Δ/R . It is found that ξ_h increases and \tilde{r}_h decreases monotonically. The

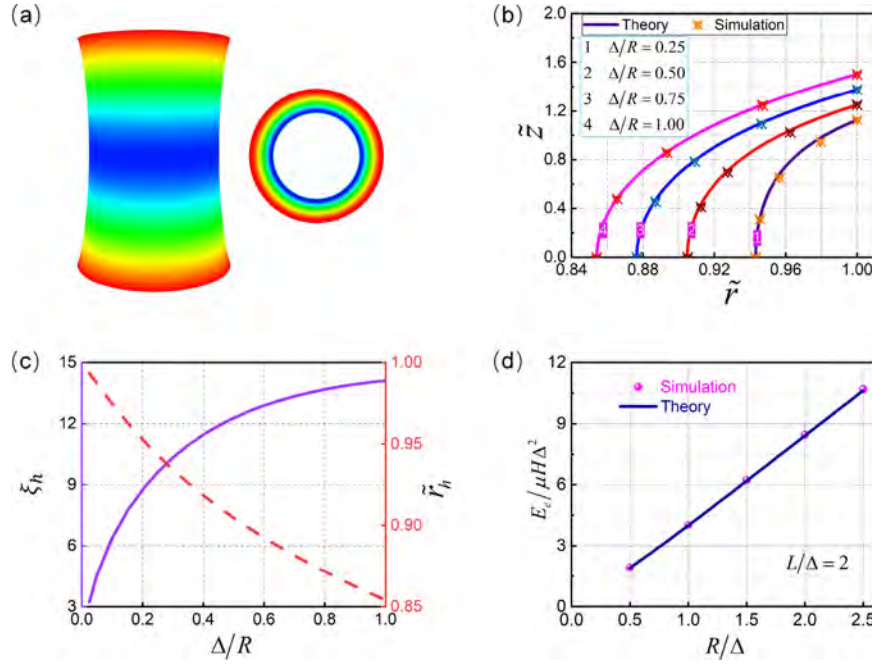


Fig. 3. Theoretical analysis and FE simulation results for film stretching. (a) Front view and top view snapshots of film from FE simulation. (b) Curves of \tilde{z} varying with \tilde{r} for different Δ/R . (c) The radius (\tilde{r}_h) at the throat and ξ_h at the top end of film versus Δ/R . (d) The dimensionless strain energy $E_e/\mu H \Delta^2$ versus R/Δ with $\eta = 2$.

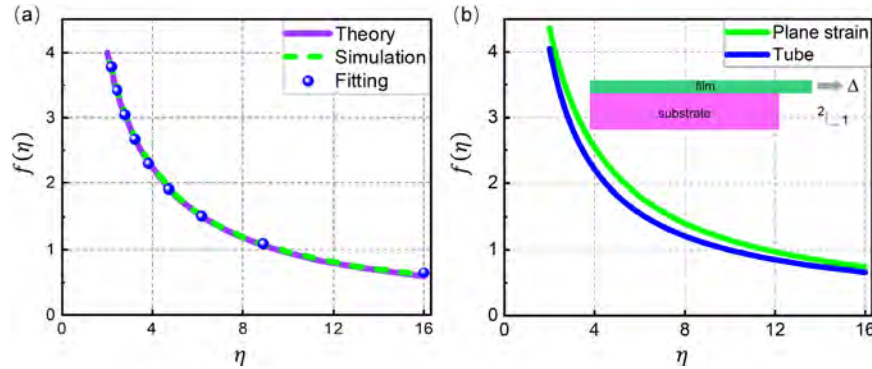


Fig. 4. The curves of $f(\eta)$: (a) from theoretical analysis, FE simulation and fitting of theoretical result, and (b) from tube and plane strain condition.

curves of dimensionless energy $E_e/\mu H \Delta^2$ varying with R/Δ are shown in Fig. 3(d) where we take $L = 40$, $\Delta = 20$ and $R = 10, 20, 30, 40, 50$. From both theoretical and FE results, E_e varies linearly with R , then a simplified form of E_e in Eq. (11) is obtained.

We now ascertain the form of $f(\eta)$ from Eq. (11). $f(\eta)$ varying with η are shown in Fig. 4(a) via both theoretical analysis and FE simulations, and they match well with each other. A suitable function is chosen to fit the theoretical curve $f(\eta)$,

$$f(\eta) = a\eta^b, \quad (16)$$

where a and b is determined as $a = 7.423$, $b = -0.874$. It can be found that $f(\eta)$ and its derivative $f'(\eta)$ monotonously decrease with η . When η approaches infinity, meaning $\Delta = 0$, $f(\eta)$ tends to zero corresponding to the case that film is in undeformed state and $E_e = 0$. When η approaches zero, namely $\Delta \rightarrow \infty$, and $f(\eta)$ approaches infinity which means that the stretching of film is infinity and $E_e \rightarrow \infty$.

When the radius R goes to infinity, the geometry of the undeformed tubular film becomes flat. A question arises that would $f(\eta)$ for tubes be degenerated to plane strain solution. In order to answer this question, it is necessary to study the case of plane

strain deformation, as shown in the inset of Fig. 4(b). Considering material incompressibility, the stretch ratios of three principle directions are $\lambda_1 = 1 + 1/\eta$, $\lambda_2 = 1/\lambda_1$ and $\lambda_3 = 1$, along stretch direction, thickness direction, and the normal direction of the plane, respectively. From Eq. (7), the plane strain energy density W^{PE} can be written as

$$W^{PE} = \frac{\mu}{2} \left(\lambda_1^2 + \frac{1}{\lambda_1^2} - 2 \right). \quad (17)$$

The total energy of the entire film is

$$E_e^{PE} = 2\pi RHLW^{PE} \quad (18)$$

Comparing with the form of Eq. (11), a similar function $f^{PE}(\eta)$ for plane strain deformation can be obtained from Eq. (18),

$$f^{PE}(\eta) = \pi \eta \left[\left(1 + \frac{1}{\eta} \right)^2 + \frac{1}{\left(1 + \frac{1}{\eta} \right)^2} - 2 \right]. \quad (19)$$

Fig. 4(b) shows the curves of Eqs. (16) and (19), and they have similar trends and both $f(\eta)$ decrease with η . However, $f(\eta)$ for

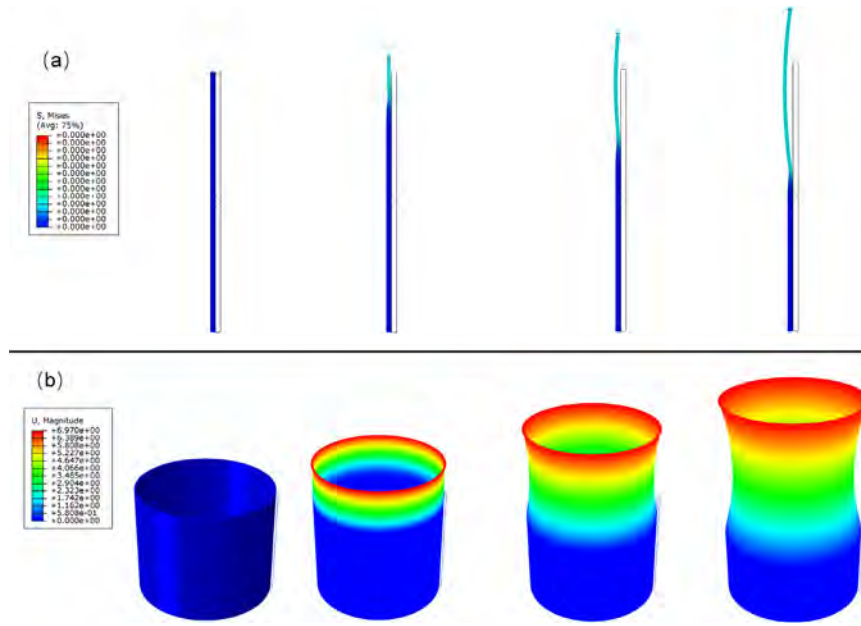


Fig. 5. Snapshots of film under different displacement: (a) axisymmetrical view, (b) view of 360 degrees rotation.

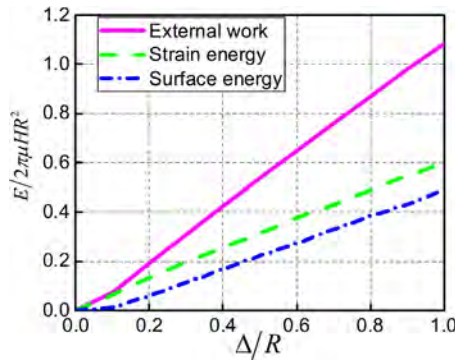


Fig. 6. Curves of external work, strain energy and surface energy from FE simulation during film peeling process.

tubes are always smaller than the one for plane-strain case, which means that the results for tubular films cannot be degenerated to the plane strain case when $R \rightarrow \infty$. The main reason is that necking causes the film to deviate from its initial surface, which makes this problem totally different from the plane-strain problem, even when the radius goes to infinity.

5.2. Film peeling results

The peeling process of tubular film is performed by FE simulation. The film with length $L_0 = 50$ and radius $R = 10$ is initially bonded to the inner surface of a rigid tube. Axisymmetric snapshots of finite element model with various Δ are shown in Fig. 5. As expected, film necking occurs in the detached region, which leads to non-zero peeling angle at the crack tip. The presence of peeling angle makes the film be peeled from tube easier. Fig. 6 shows the FE simulation curves of external work, strain energy, and surface energy during tubular film peeling. When the displacement Δ/R is small, the crack will not propagate and surface energy is equal to 0, which implies the external work is all converted into strain energy of the film. Once the crack propagation criterion is satisfied, the external work will be converted into strain energy and surface energy. From the

definition of the energy release rate G in Eq. (14), we obtain $G = 0.244$ from the curves shown in Fig. 6.

Substituting the obtained function of $f(\eta)$ in Eq. (16) into Eq. (15), the theoretical crack propagation criterion can be explicitly given

$$\eta = \frac{L}{\Delta} = \left(-\frac{2\pi G}{ab\mu H} \right)^{\frac{1}{b-1}}. \quad (20)$$

It is obviously that the crack length L varies linearly with the applied displacement Δ during peeling process. For a given tubular peeling system with a crack length L , when the stretch loading Δ exceeds L/η , the crack expands until the crack propagation criterion (15) satisfied. Fig. 7(a) shows the curves of L linearly varying with Δ from theoretical analysis and FE simulation. The slope of theoretical curve is 2.183, while the slope of simulation curve is 2.175. They are very close.

Then we study the force F needed at the top of the film. In our theoretical model, F can be obtained by integrating the axial stress at the top end,

$$F = \frac{2\pi RH\sigma_s \cos \xi}{\lambda_\theta \lambda_s}. \quad (21)$$

In FE simulation, the F can be extracted as the reaction force of the top end. Fig. 7(b) shows the curves of dimensionless force $F/2\pi\mu RH$ versus Δ/R . The linear segment at the beginning represents the film stretching without peeling, which is caused by the initial crack setting. Note that there is a sudden wave in $F/2\pi\mu RH$ when the crack start to propagate, which may be caused by the transformation of two states of film. Then, $F/2\pi\mu RH$ slightly decreases with the displacement loading.

5.3. Measurement of adhesion properties

Determination of adhesion properties is one of the crucial subjects of soft matter. The adhesion property is assessed by mechanical tests [29] and peeling test is a typical one. In this test, a common relationship between the strength of the adhesion Γ and peeling angle β as well as the steady force F_{ss} can be defined as $\Gamma = F_{ss}/h_0(1 - \cos \beta)$, where h_0 is the width of the adhesion region [30]. However, it can be seen that this equation

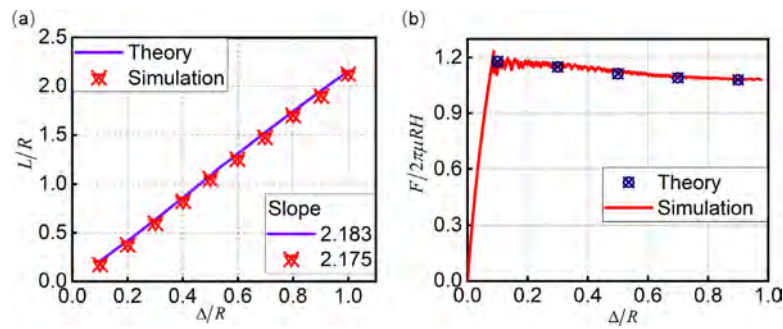


Fig. 7. (a) The dimensionless peeling stretch vs. displacement of top of film. (b) The dimensionless pull force vs. displacement of top of film.

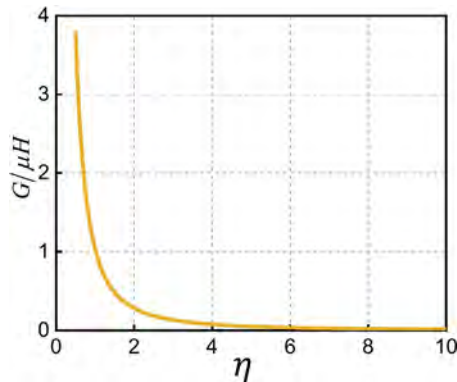


Fig. 8. The dimensionless critical energy release rate vs. η .

becomes singular when the peeling angle is close to 0. The results of the literature [31] show that there are two deformation modes that film peeling from a plate with zero peeling angle. When the length of the glued region is short, the peeling is completed instantly as the force increases. When the glued region is long, the elastomer peels from the substrate as the peeling force reaches a limit value, which is independent of the length of glued region. The peculiarity of peeling behavior with zero peeling angle makes it difficult to carry out in experiments. As mentioned in literature [32], a further restriction on $F_{ss}/h_0(1 - \cos \beta)$ is that the peeling angle should be sufficiently large such that the denominator does not approach zero. In addition, peeling force may theoretically diverge at vanishing peeling angle, due to the presence of sliding friction at the interface [22]. Consequently, in peeling tests, common peeling angles are $\pi/2$ and π with force controlled loading mode.

The advantage of flat film peeling experimental setup with zero peeling angle is that the directions of external force and displacement are the same, which is one degree of freedom loading mode and allows the adhesion property of film–substrate system to be tested by tensile machine. A one degree of freedom peeling test with no theoretical divergence is essential to ascertain the adhesion property of film–substrate. From results of our work, tubular film peeling can satisfy this requirement due to the existing of non-zero tip angle, and could be used to measure the surface properties. From Eq. (15), we can obtain G as

$$\frac{G}{\mu H} = -\frac{ab}{2\pi} \eta^{b-1}. \quad (22)$$

According to Eq. (22), a simple experimental setup can be described below: First, a film is bonded to inner tube surface with a short length of the film outside the tube to form an initial crack. Then, the film top end is fixed to a rigid rod with the same radius of tube. Finally, the rod is stretched along axial direction

at a constant displacement loading rate. We can record the crack length L and Δ . Recorded crack length L is the initial crack length plus the distance between the crack and the top of the tube, so the length of the film outside the tube does not affect the results. The adhesion G can be estimated by substituting L and Δ into Eq. (22) with the geometry parameters μ and H . Fig. 8 shows the results of Eq. (22), where G monotonically decreases with η . The monotonous property guarantees that the estimated G can be directly solved from Eq. (22) by measuring L and Δ .

6. Conclusion

Peeling behaviors of elastic films bonded to tubular surfaces have been studied via theoretical analysis and finite element simulations. Based on the non-linear elastic theory and energy-based fracture criterion, we have established an axisymmetric finite deformation model to study axial stretching behaviors of films with one end glued onto an inner tube and the other end fixed with a rigid ring, resulting expected film necking effects. We have employed dimensional analysis to study the film free energy. In addition, we have studied film peeling behaviors from tubular surfaces under the displacement controlled loading mode, manifesting that the direction of loading and film displacement is the same. Key findings of this work include:

- (1) For film stretching, the relationship between the elastic film strain energy and material properties, geometric parameters, and loading parameters is derived.
- (2) Base on the film stretching strain energy, the crack propagation criterion of the film part glued onto tubular surfaces has been obtained, showing that there is a linear relationship between the crack length and displacement load.
- (3) Compared to planar zero degree peeling angle methods, our solution has decoupled the surface frictions due to the film necking, which has shown significant benefit and convenience for theoretical analysis and experiments using only one degree of freedom stretching.

This work also provides a new methodology for studying and testing of adhesion properties of soft matter under large deformations. Future work includes but is not limited to 3D simulations and experiments under complex loading conditions.

Declaration of competing interest

The authors declare that they have no known competing financial interests or personal relationships that could have appeared to influence the work reported in this paper.

Data availability

No data was used for the research described in the article.

Acknowledgments

This work is supported by the science foundation of national key laboratory of science and technology on advanced composites in special environments and the Heilongjiang Touyan Innovation Team Program.

References

- [1] A.A. Khalili, M.R. Ahmad, A review of cell adhesion studies for biomedical and biological applications, *Int. J. Mol. Sci.* 16 (8) (2015) 18149–18184.
- [2] Z. Szekanecz, A.E. Koch, Endothelial cells and immune cell migration, *Arthritis Res. Ther.* 2 (5) (2000) 1–6.
- [3] T. Okegawa, R.-C. Pong, Y. Li, J.-T. Hsieh, The role of cell adhesion molecule in cancer progression and its application in cancer therapy, *Acta Biochim. Pol.* 51 (2) (2004) 445–457.
- [4] H. Perinpanayagam, R. Zaharias, C. Stanford, R. Brand, J. Keller, G. Schneider, Early cell adhesion events differ between osteoporotic and non-osteoporotic osteoblasts, *J. Orthop. Res.* 19 (6) (2001) 993–1000.
- [5] X. Sun, L. Yu, M. Rentschler, H. Wu, R. Long, Delamination of a rigid punch from an elastic substrate under normal and shear forces, *J. Mech. Phys. Solids* 122 (2019) 141–160.
- [6] M. Susoff, K. Siegmann, C. Pfaffenroth, M. Hirayama, Evaluation of icephobic coatings—Screening of different coatings and influence of roughness, *Appl. Surf. Sci.* 282 (2013) 870–879.
- [7] S.T. Zhang, H. Wang, L. Wang, Progress in ice-phobic coating, in: *Advanced Materials Research*, Vol. 399, Trans Tech Publ, 2012, pp. 2044–2048.
- [8] H. Yuk, C.E. Varela, C.S. Nabzdyk, X. Mao, R.F. Padera, E.T. Roche, X. Zhao, Dry double-sided tape for adhesion of wet tissues and devices, *Nature* 575 (7781) (2019) 169–174.
- [9] A. Kleinbichler, M. Bartosik, B. Völker, M.J. Cordill, Thin film adhesion of flexible electronics influenced by interlayers, *Adv. Eng. Mater.* 19 (4) (2017) 1600665.
- [10] K. Kendall, Thin-film peeling—the elastic term, *J. Phys. D: Appl. Phys.* 8 (13) (1975) 1449.
- [11] A. Molinari, G. Ravichandran, Peeling of elastic tapes: effects of large deformations, pre-straining, and of a peel-zone model, *J. Adhes.* 84 (12) (2008) 961–995.
- [12] M. Loukis, N. Aravas, The effects of viscoelasticity in the peeling of polymeric films, *J. Adhes.* 35 (1) (1991) 7–22.
- [13] K.-S. Kim, J. Kim, Elasto-plastic analysis of the peel test for thin film adhesion, 1988.
- [14] L. Afferrante, G. Carbone, The ultratough peeling of elastic tapes from viscoelastic substrates, *J. Mech. Phys. Solids* 96 (2016) 223–234.
- [15] Z. Peng, S. Chen, A. Soh, Peeling behavior of a bio-inspired nano-film on a substrate, *Int. J. Solids Struct.* 47 (14–15) (2010) 1952–1960.
- [16] Z. Peng, S. Chen, Peeling behavior of a thin-film on a corrugated surface, *Int. J. Solids Struct.* 60 (2015) 60–65.
- [17] W. Deng, H. Kesari, Angle-independent optimal adhesion in plane peeling of thin elastic films at large surface roughnesses, *J. Mech. Phys. Solids* 148 (2021) 104270.
- [18] H.-P. Zhao, Y. Wang, B.-W. Li, X.-Q. Feng, Improvement of the peeling strength of thin films by a bioinspired hierarchical interface, *Int. J. Appl. Mech.* 5 (02) (2013) 1350012.
- [19] O. Kruglova, F. Brau, D. Villers, P. Damman, How geometry controls the tearing of adhesive thin films on curved surfaces, *Phys. Rev. Lett.* 107 (16) (2011) 164303.
- [20] L. Brely, F. Bosia, N.M. Pugno, The influence of substrate roughness, patterning, curvature, and compliance in peeling problems, *Bioinspiration Biomim.* 13 (2) (2018) 026004.
- [21] Ş. Çitil, İ. Bozkurt, M.D. Aydın, Experimental and 3D non-linear stress analysis of adhesively bonded pipes with curved-surface lap joints, *J. Adhes.* 95 (5–7) (2019) 515–528.
- [22] M. Ceglie, N. Menga, G. Carbone, The role of interfacial friction on the peeling of thin viscoelastic tapes, *J. Mech. Phys. Solids* 159 (2022) 104706.
- [23] C.B. Haverkamp, D. Hwang, C. Lee, M.D. Bartlett, Deterministic control of adhesive crack propagation through jamming based switchable adhesives, *Soft Matter* 17 (7) (2021) 1731–1737.
- [24] A.M. Kolesnikov, N.Y. Shubchinskaya, Cylindrical membrane partially dressed on a rigid body of revolution, *Contin. Mech. Thermodyn.* 33 (4) (2021) 1331–1346.
- [25] A.M. Kolesnikov, Cylindrical membrane partially stretched on a rigid cylinder, *Int. J. Non-Linear Mech.* 86 (2016) 15–22.
- [26] R. Dickey, Stretching of cylindrical membranes, *Int. J. Non-Linear Mech.* 5 (1) (1970) 35–43.
- [27] R.W. Ogden, *Non-Linear Elastic Deformations*, Courier Corporation, 1997.
- [28] S.P. Pearce, J.R. King, M.J. Holdsworth, Axisymmetric indentation of curved elastic membranes by a convex rigid indenter, *Int. J. Non-Linear Mech.* 46 (9) (2011) 1128–1138.
- [29] Y. Wang, X. Yang, G. Nian, Z. Suo, Strength and toughness of adhesion of soft materials measured in lap shear, *J. Mech. Phys. Solids* 143 (2020) 103988.
- [30] J. Liu, S. Qu, Z. Suo, W. Yang, Functional hydrogel coatings, *Natl. Sci. Rev.* 8 (2) (2021) nwa254.
- [31] S. Ponce, J. Bico, B. Roman, Effect of friction on the peeling test at zero-degrees, *Soft Matter* 11 (48) (2015) 9281–9290.
- [32] J.A. Williams, J.J. Kauzlarich, The influence of peel angle on the mechanics of peeling flexible adherends with arbitrary load–extension characteristics, *Tribol. Int.* 38 (11–12) (2005) 951–958.